

Nonlinear optical approach to matrix-element spectroscopy of the $5s\ ^2S_{1/2} \rightarrow 5p\ ^2P_j \rightarrow 5d\ ^2D_{j'}$ transitions in ^{87}Rb

S B Bayram¹, M D Havey², M S Safronova³ and A Sieradzan⁴

¹ Physics Department, Miami University, Oxford, OH 45056, USA

² Department of Physics, Old Dominion University, Norfolk, VA 23529, USA

³ Department of Physics and Astronomy, University of Delaware, Newark, DE 19716, USA

⁴ Physics Department, Central Michigan University, Mt Pleasant, MI 48859, USA

E-mail: bayramsb@muohio.edu, mhavey@odu.edu, msafro@udel.edu and andy@phy.cmich.edu

Received 1 March 2006, in final form 12 April 2006

Published 15 May 2006

Online at stacks.iop.org/JPhysB/39/2545

Abstract

We present in this paper results of a nonlinear optical spectroscopy approach to measurement of excited-state transition matrix elements. Recent advances in the quality of excited-state transition matrix elements have permitted renormalization of earlier measurements of transition amplitudes associated with the $5s\ ^2S_{1/2} \rightarrow 5p\ ^2P_j \rightarrow 5d\ ^2D_{3/2}$ two-photon transitions in atomic ^{87}Rb . Previous measurements were made to high precision, but further improvement of the accuracy was limited by uncertainties in data describing the influence of energetically distant transitions. Availability of more reliable matrix elements, including relativistic all-order calculations of transition matrix elements in alkali atoms, has since significantly improved the situation. In the present paper, we show that theoretical relative transition amplitudes for the excited state $5p\ ^2P_j \rightarrow 5d\ ^2D_{3/2}$ doublet (ratio = 1.098(9)) are now in excellent agreement with experiment (ratio = 1.090(6)). This result, combined with our recent work on caesium, shows that it is possible to determine relative line strengths, for transitions connecting atomic excited states, with precision previously found only in state-of-the-art measurements of alkali resonance doublets. Detailed discussion of the experimental technique and supporting data, including polarization measurements on the $5s\ ^2S_{1/2} \rightarrow 5p\ ^2P_j \rightarrow 5d\ ^2D_{5/2}$ transitions, is also presented.

(Some figures in this article are in colour only in the electronic version)

1. Introduction

Precise determination of atomic transition probabilities has been an important task for experimental and theoretical atomic physicists [1–6]. Over the past few years a series of high-precision results has been reported, mostly for principal series transitions involving the atomic ground state of alkali atoms [7–17]. A good example of this is the resonance 6s–6p doublet of the caesium atom, where atomic lifetimes [12–14], direct absorption measurements [15, 16], light scattering studies [18], determination of van der Waals C_3 coefficients and polarizability measurements have produced a highly accurate [19–21], and nearly internally consistent [22], set of data in generally excellent agreement with theory. Although transitions between excited states are of similar, or even greater, interest they have been much less studied by experimentalists, in part because the methods developed for the principal series are not readily applicable in a more general case.

To address this problem, we have developed a nonlinear optical spectroscopy approach, two-photon, two-colour polarization spectroscopy, and applied it to precision measurements of atomic transition probabilities and hyperfine structure in Na, K, Rb and Cs [18, 23–26]. Although two-photon spectroscopy has been used for precision measurements of atomic and molecular line positions, we emphasize here that it is also applicable to measurement of other atomic properties as well. In fact, in previous work, we have shown that it is quite suitable for measurements concerning transitions connecting excited atomic states. Among the reasons for this is that the approach represents a mapping of transition matrix elements into the frequency domain [27], and that the relevant frequency and polarization observables can be determined robustly, free of many common systematic effects. However, until recently the experimental data and a sharp comparison with theoretical results could not be fully developed. This was primarily due to the fact that, in all cases, the transition amplitudes under investigation contained contributions from energetically distant levels. A strict comparison with theory for a given transition was impossible, unless corrections for all significant additional contributions could be reliably made. Even so, it has been possible to find, in the form of polarization-dependent sum rules, certain constraints on the transition matrix elements [24]. Alternatively, the experimental result had to be interpreted as an overall measure of the relative two-photon transition amplitudes, a quantity not typically calculated to very high accuracy.

Over the past few years, a quite large set of sophisticated and generally accurate theoretical matrix-element calculations has become available. These values are of sufficient accuracy to make the necessary adjustments to the experimental measurements to obtain transition matrix-element ratios to a relative precision of 10^{-3} or better. It is important to realize that, in this approach, the off-resonance transitions typically contribute only a few per cent to the experimental measurements. Thus, theoretical values reliable to 10% are frequently sufficient to make corrections of the required precision. This type of full analysis of frequency-dependent polarization spectroscopy data, accompanied by a direct comparison with theory, has recently been demonstrated in a detailed study of the $6p\ ^2P_j \rightarrow 8s\ ^2S_{1/2}$ doublet in atomic Cs [26].

Motivated by this result, we have revisited our experimental data associated with earlier measurements of the $5p\ ^2P_j \rightarrow 5d\ ^2D_{3/2}$ excited doublet transition in Rb; contributions from off-resonance transitions had only been estimated in that earlier work. We point out here a particular interest in this transition: the correlation correction to $5d\ ^2D_{3/2}$ – $5p\ ^2P_{3/2}$ and $5d\ ^2D_{3/2}$ – $5p\ ^2P_{1/2}$ electric-dipole matrix elements and their ratio is extremely large. Therefore, these transitions represent an excellent test of the high-precision methods of the current state-of-the-art atomic theory. As we will see, improvements in the theoretical results and inclusion of off-resonance transitions now yield an experimental excited-state matrix-element ratio of 1.090(6), in excellent agreement with the all-order relativistic theoretical ratio of 1.098(9).

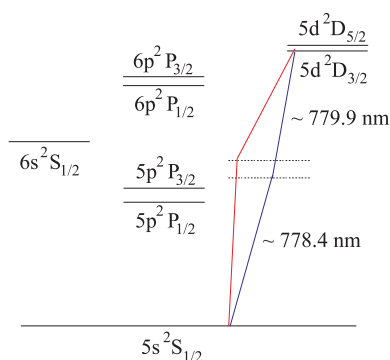


Figure 1. Energy level diagram for selected low-lying excited electronic states in atomic Rb. The different excitation pathways for two-photon excitation, and the approximate vacuum wavelength of the two light sources, are also shown.

A similar reinterpretation procedure could be applied to other cases as well. Finally, we point out for clarity that there are two types of theoretical data that are considered in this approach. In the first, excited-state transition matrix elements for a wide range of transitions are used. These data may come from relativistic Hartree–Fock calculations, for example. Lower precision is generally acceptable in these data, which are used to make higher-order modification of experimental results. In the second, fully relativistic all-order calculations of selected transition elements are employed using the most sophisticated relativistic atomic many-body techniques available. It is these values that are directly compared with the adjusted experimental matrix-element ratio.

In the present paper, we first reiterate the experimental technique, systematic effects and core matrix-element measurements. To illustrate some of the effects, we present additional data involving the $5d^2D_{5/2}$ final level. The procedure and theoretical data used to account for off-resonance transitions are then presented. This is followed by a description of the all-order relativistic calculation for the present case and a comparison of the revised experimental and theoretical results.

2. Experimental approach

The experimental scheme, as applied to the case considered here, is illustrated in figure 1. In general, a two-colour two-photon transition is induced between the atomic ground level and a selected higher lying excited level. Two separately tuneable lasers are used for that purpose. Their frequencies, ω_{11} and ω_{12} , are adjusted independently, but in such a way that the sum satisfies the two-photon resonance condition. For future reference, we define the detuning of laser 1 from the $5s^2S_{1/2} \rightarrow 5p^2P_{3/2}$ resonance as $\Delta_1 = \omega_{11} - \omega_{5p_{3/2}}$. In accordance with lowest order perturbation theory, the excitation efficiency scales as the detuning between the virtual and the nearest real level corresponding to a single-photon resonance. If the virtual level lies in the vicinity of multiplet atomic levels, rather than a single level, more than one multiplet member may contribute to the overall transition amplitude. Since these contributions add with generally different phases and magnitudes, interesting interference effects are expected, including sharp minima in the two-photon transition probability for certain detunings. The locations of those minima, as well as the overall shape of the excitation versus detuning curve, depend sensitively on the transition matrix elements corresponding to the allowed excitation

paths and can be used for their determination. In the present case, and in the electric-dipole approximation, the relative polarization-dependent two-photon transition amplitude is given by [4, 28]

$$\sum_n \left[\frac{\langle \Psi_f | \epsilon_1 \cdot r | \Psi_n \rangle \langle \Psi_n | \epsilon_2 \cdot r | \Psi_i \rangle}{\omega_n - \omega_{11}} + \frac{\langle \Psi_f | \epsilon_2 \cdot r | \Psi_n \rangle \langle \Psi_n | \epsilon_1 \cdot r | \Psi_i \rangle}{\omega_n - \omega_{12}} \right]. \quad (1)$$

In this expression, ϵ_k and ω_{1k} represent the polarization vector and the frequency of the light source ($k = 1, 2$). The index n labels the contributing intermediate levels and their frequencies ω_n . In the present case, where we consider the atomic Rb $5s \ ^2S_{1/2} \rightarrow 5d \ ^2D_j$ two-photon transition, the dominant terms in the amplitude expression are those connecting initial and final states with resonant P states as intermediaries. Since transition amplitudes associated with the resonant doublet are known to a high accuracy, the relative amplitudes for transitions connecting the final excited level with the P levels may be determined by analysing the excitation rate dependence on detuning. Complications arise from the fact that there are two so-called virtual levels associated with the two-photon transition, which correspond to two possible orders of photon absorption, and from contributions from far-off-resonance levels. However, as demonstrated in our most recent set of measurements on the atomic two-photon Cs $6s \ ^2S_{1/2} \rightarrow 8s \ ^2S_{1/2}$ transition, very accurate determinations of relative transition amplitudes within excited multiplets may still be obtained.

From a practical point of view, direct measurement of excitation efficiency is a poor strategy. Frequency and power drifts of the laser sources, fluctuations and spatial gradients of the cell temperature and instabilities in beam directionality may adversely affect the intensity readings. To minimize these errors, it is advantageous to deal with relative, rather than absolute, excitation probabilities. In our experiments to date, the preferred quantity for experimental determination is the linear polarization degree, defined by

$$P_L = \frac{I_{\parallel} - I_{\perp}}{I_{\parallel} + I_{\perp}}. \quad (2)$$

In formula (2), I_{\parallel} and I_{\perp} represent two-photon-induced populations obtained with laser beams being linearly polarized, with polarization vectors either parallel or perpendicular to each other. We point out that in general any two different polarization states may be used. For the case we are considering here, $5s \ ^2S_{1/2} \rightarrow 5p \ ^2P_j \rightarrow 5d \ ^2D_{3/2}$, with $j = 1/2, 3/2$, expressions for orthogonal linear polarizations of the exciting laser sources are given by equations (2)–(7). These equations ignore the influence of hyperfine structure which, depending on the transition considered, modifies the numerical coefficients:

$$I_{\parallel} = \left[\frac{5}{\omega_{11} - \omega_{1/2}} + \frac{5}{\omega_{12} - \omega_{1/2}} + \frac{R}{\omega_{11} - \omega_{3/2}} + \frac{R}{\omega_{12} - \omega_{3/2}} + p \right]^2, \quad (3)$$

$$I_{\perp} = I_{1\perp} + I_{2\perp} \quad (4)$$

where

$$I_{1\perp} = \frac{3}{4} \left[\frac{-5}{\omega_{11} - \omega_{1/2}} + \frac{2R}{\omega_{11} - \omega_{3/2}} - \frac{3R}{\omega_{12} - \omega_{3/2}} + q_1 \right]^2, \quad (5)$$

$$I_{2\perp} = \frac{25}{4} \left[\frac{1}{\omega_{11} - \omega_{1/2}} + \frac{2}{\omega_{12} - \omega_{1/2}} + \frac{4R/5}{\omega_{11} - \omega_{3/2}} - \frac{R/5}{\omega_{12} - \omega_{3/2}} + q_2 \right]^2, \quad (6)$$

$$R = \frac{\langle 5d_{3/2} \| d \| 5p_{3/2} \rangle \langle 5p_{3/2} \| d \| 5s \rangle}{\langle 5d_{3/2} \| d \| 5p_{1/2} \rangle \langle 5p_{1/2} \| d \| 5s \rangle}. \quad (7)$$

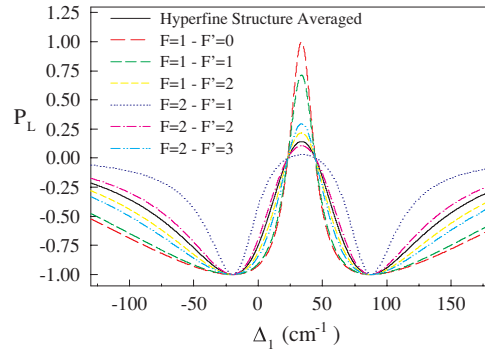


Figure 2. Detuning and hyperfine level dependence of the linear polarization degree of the $5s\ ^2S_{1/2} \rightarrow 5d\ ^2D_{3/2}$ two-photon transition. Detunings are measured in cm^{-1} units of the laser 1 frequency from the $5s\ ^2S_{1/2} \rightarrow 5p\ ^2P_{3/2}$ transition.

In this definition of the reduced matrix-element ratio R , corresponding values of the C_1 reduced matrix elements, where C_1 represents the normalized spherical harmonics, are explicitly evaluated in the intensity formulae. That is, all the matrix elements in equations (7)–(9) are divided by the corresponding C_1 matrix elements [29]. This procedure makes clear the relativistic effects on the reduced matrix elements.

In all expressions, d is the electric-dipole operator. In the intensity expressions, the quantities p , q_1 and q_2 , which represent sums over np multiplets with $n > 5$, have the same form as the remaining terms in each bracket, but with the resonance frequencies and matrix elements referred to the np levels with $n > 5$. Here, $\omega_{1,12}$ labels the frequency of the absorbed photons. The resonance frequencies for the $5s\ ^2S_{1/2} \rightarrow 5p\ ^2P_j$ transitions are explicitly labelled as ω_j , where $j = 1/2, 3/2$.

In addition, the matrix-element ratio R can be usefully factored as a product $R_2 R_1$ of ratios of matrix elements, as defined in equations (8) and (9). The portion representing the contribution from the resonance transition,

$$R_1 = \frac{\langle 5p_{3/2} \| d \| 5s \rangle}{\langle 5p_{1/2} \| d \| 5s \rangle}, \quad (8)$$

has the well-known value of $R_1 = 0.999(1)$ as determined from precise measurements on this transition. We are then focused in this work on the excited-state ratio

$$R_2 = \frac{\langle 5d_{3/2} \| d \| 5p_{3/2} \rangle}{\langle 5d_{3/2} \| d \| 5p_{1/2} \rangle}. \quad (9)$$

Finally, we point out that the above expressions apply to the case where the hyperfine interaction may be ignored. However, even when the detuning from the intermediate P levels is large, the resulting polarization depends strongly on the selection of individual initial and final hyperfine levels. We present in figure 2 the dependence of P_L on detuning and on hyperfine level. There we see that the polarization degree varies from +1.0 to -1.0 over a fairly small range of detunings. As discussed in a later section of this paper, the strong variation of the polarization degree with detuning has an effect on the measured polarization, even over the profile of an individual two-photon resonance.

Even with signals for each polarization state sensitive to the various systematic effects mentioned above, P_L is not, as long as measurements corresponding to different polarizations are taken repeatedly in quick succession. Data analysis involves determining theoretical

expressions for the polarization P_L in terms of atomic transition matrix elements and fitting its experimental dependence on detuning, with the matrix-element ratio as an adjustable parameter. With polarizations at specific detunings determined to a fraction of a per cent, a least-squares fitting procedure can readily provide $\sim 10^{-3}$ accuracy on relative transition amplitudes.

2.1. Some systematic effects in matrix-element spectroscopy

We discuss in this section some physical effects which must be treated with care in order to achieve the full potential of the method. The technique is based on comparison of two-photon excitation rates obtained for different relative polarizations of two laser beams. The number of atoms brought to the final state is generally polarization dependent, and the corresponding reduced signal is given as a ratio of experimentally derived fluorescence intensities, $P_m = (S_1 - S_2)/(S_1 + S_2)$. This expression is the analogue of equation (2), with the quantities S referring to the signals in each polarization channel. In this expression, the labels 1 and 2 refer to different polarization states of the exciting laser beams. In our measurements, these have the indicated two orthogonal linear polarization states, but states of general elliptical polarization may be advantageous. The quantity P_m can be expressed directly in terms of relative matrix elements, as illustrated in equations (3)–(10); these formulae normally contain larger terms arising from quasi-resonance transitions, and summations of many smaller terms coming from energetically more distant states. For non-resonant two-photon transitions, the measured intensities and the ratio are insensitive to collisions, radiation trapping and to FM noise in the excitation frequency. Further, as the exciting laser beams may be aligned to a diffraction-limited level, angular dispersion of the measured polarization becomes entirely negligible. The polarization dependence then is limited by the quality of polarizing elements that are used to define the polarization state of the lasers and the birefringent properties of the atomic vapour and the cell windows. The two-photon excited level population is obtained from the intensity of fluorescence from that state (or its cascade). Here, one must remember that the final fluorescing level may possess electronic polarization and its fluorescence intensity distribution may not be isotropic. This presents a difficulty in comparisons between ideal theoretical expressions and the measured polarization observables.

Several solutions to this problem have been proposed and experimentally examined. These include: (a) integrating the fluorescence over the full spherical angle, (b) using a magic angle polarizer in the detection arm and (c) allowing collisions or radiation diffusion to depolarize the fluorescing level (by working with higher density vapours). In our experiments to date, the third approach has been found the best from a practical and signal-to-noise point of view. The final state polarization effects and their elimination have been clearly demonstrated in the rubidium experiment. To illustrate these points, note that the two-photon transition amplitude to the $5d\ ^2D_{5/2}$ state has, as intermediate states, np levels with angular momentum $j = 3/2$ only (corresponding to the $5s\ ^2S_{1/2} \rightarrow np\ ^2P_{3/2} \rightarrow 5d\ ^2D_{5/2}$ path), P_L should be exactly $1/7$ (14.3%) for all detunings. However, the experimental data obtained at lower Rb vapour densities show substantial deviation from that value, most likely as a result of electronic polarization of the fluorescing $6p\ ^2P_{3/2}$ level. The source of this alignment is the optical-excitation-induced polarization of the $5d\ ^2D_{5/2}$ level, which is partly transferred by cascade to the $6p\ ^2P_{3/2}$ level. As discussed below, the size of this effect is consistent with calculations based on the alignment of the original level and the competing effect of hyperfine depolarization of the alignment in each level. As shown in figure 2, this deviation disappears as the cell temperature is raised and depolarization due to radiation trapping and collisions

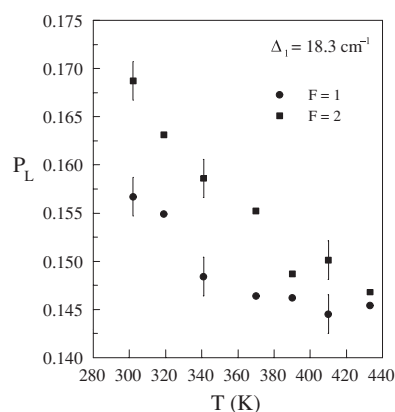


Figure 3. Cell temperature dependence of cascade fluorescence polarization on the $6p\ ^2P_{3/2} \rightarrow 5s\ ^2S_{1/2}$ transition. Excitation in this case was to the final $5d\ ^2D_{5/2}$ level. Asymptotic approach to the theoretically expected polarization degree of 14.3% is clearly seen.

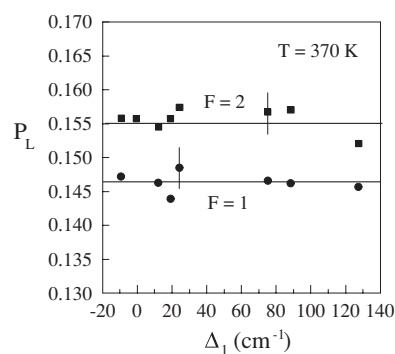


Figure 4. Detuning and initial hyperfine level dependence of the linear polarization degree for the $5s\ ^2S_{1/2} \rightarrow 5p\ ^2P_j \rightarrow 5d\ ^2D_{5/2}$ transition. Experimental data for the $F = 1$ and the $F = 2$ ground initial hyperfine levels are shown. These data were taken at a temperature of 370 K.

sets in. One can see that around 400 K polarization readings come to closely agree with the 14.3% prediction, within the limits of experimental error.

Another interesting feature of the polarization data is the difference between the low temperature results obtained for transitions originating in different hyperfine components of the electronic ground level. This is illustrated for the $5d\ ^2D_{5/2}$ final level in figure 3, where it is seen that excitation from the $F = 2$ level produces consistently higher measured polarization values. As shown in figure 4, this result does not depend on the detuning from the intermediate levels of the two-photon transition. To understand general features of final state polarization effects in more quantitative terms, we consider a straightforward theoretical model and apply it to atoms with alkali-metal atom structure. Initially, we ignore effects due to hyperfine coupling. Assuming that atoms entering the laser beams have no initial electronic polarization, we use two-photon transition amplitudes (namely, equation (1)) between $|j, m_j\rangle$ states to obtain populations in the m_j states of the $5d\ ^2D_{5/2}$ level. Subsequently, electric-dipole selection rules are applied to $5d\ ^2D_{5/2} \rightarrow 6p\ ^2P_{3/2}$ step to obtain m_j populations in the

fluorescing $6p\ ^2P_{3/2}$ level. These, together with any Zeeman coherences, define the spatial distribution of the fluorescence signal, which is the critical quantity determining the measured polarization.

For a specific application, when parallel (z - z) linear polarizations are selected for the two pumping light sources, there are no final state coherences, and the fluorescence spatial distribution is determined by the final state population distribution only. Further, because the excitation has axial symmetry, the fluorescence distribution must be rotationally symmetric about the z -axis. In the cascade to the observed fluorescing $6p\ ^2P_{3/2}$ level, the Zeeman transition strengths show a preference to populate the $|m_j| = 1/2$ substates. This, in turn, results in a relative weakness of fluorescence observed along the z -axis and a related enhancement of signals observed at right angles to the z -axis. In the geometry of the experiment, the observation direction corresponds to the y -axis, so when the measured fluorescence intensity is used to probe the populations, the relative populations are overestimated by a factor of $6/5$.

For excitation with orthogonally polarized beams we carry out the calculations for light propagating along the z -axis and polarized along the x - and y -axes. In this case, the $|m_j|$ population imbalance in the $^2P_{3/2}$ level leads to an enhanced fluorescence in the z -direction and a relatively weaker signal in the orthogonal directions. An important point is that the two lasers have quite similar frequencies, so the transition amplitudes are nearly the same for the two contributing cases where laser 1 is polarized along x , while laser 2 is polarized along y , and vice versa. Then, the signals observed along the x - and y -directions are nearly identical. For observation along either of these directions, the intensity measurements underestimate the overall populations in relation to an isotropic angular distribution. Overall, this overestimation of I_{\parallel} , along with underestimation of I_{\perp} , is responsible for an increased polarization at lower temperatures. Detailed calculations, following the approach above, leads to an apparent linear polarization degree of 33.3% (instead of 14.3% based strictly on no final state interactions).

The above considerations are modified substantially by consideration of hyperfine recoupling in the $^2D_{5/2}$ and $^2P_{3/2}$ levels. We assume full development of the hyperfine structure in each level, which is justified by the relatively long lifetime of those levels in relation to the inverse hyperfine splittings. This results in an initial hyperfine-level-dependent result of $P_L(F = 2) = 0.213$ and $P_L(F = 1) = 0.170$. Further integration of the results over the solid angle of observation leads to linear polarization degrees of 0.199 ($F = 2$) and 0.165 ($F = 1$). The results of this model are then in good semiquantitative agreement with the lower temperature experimental data.

In investigations involving the $5d\ ^2D_{3/2}$ level, on which we are primarily focused, the problem of the final state alignment did not arise, principally because the $5d\ ^2D_{3/2}$ level population cascades almost exclusively to the $5p\ ^2P_{1/2}$ level, which can support no alignment. Consistent with the physical picture just presented, P_L readings were insensitive to the temperature of the cell, as well as polarization filtering of the fluorescence signals with a magic angle polarizer. In conclusion, final state alignment effects in two-photon two-colour polarization spectroscopy are a potential significant source of systematic errors in polarization measurements, and one needs to make sure these are eliminated or corrected for, before high accuracy claims on transition amplitudes are made.

Another type of systematic error may result from mistreatment of the effects that hyperfine structure may have on the linear polarization degree. Our standard protocol for polarization measurements calls for the laser frequency of one of the sources to scan discretely over the two-photon resonance. At each frequency, signal collection is made with parallel, and then perpendicular, polarizations of the beams. A constant P_L value across the line profile can serve as evidence for internal data consistency. We first point out that what is experimentally found as a line profile depends on the arrangement of laser beams, that is if they are co-propagating

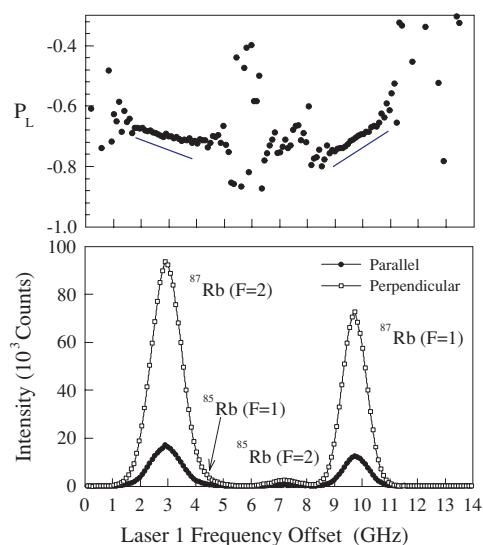


Figure 5. Excitation and linear polarization spectrum for $F = 1, 2$ hyperfine components of the $5s\ ^2S_{1/2} \rightarrow 5p\ ^2P_{3/2} \rightarrow 5d\ ^2D_{3/2}$ transition, showing the asymmetry of the measured linear polarization across the line profile. The much weaker analogous transition due to trace amounts of ^{85}Rb in the sample is also seen.

or counter-propagating. The latter geometry has the potential of nearly eliminating Doppler broadening and providing separate polarization data for individual hyperfine components of the two-photon transition, which may or may not be identical. The obvious disadvantage of using counter-propagating beams is the requirement for scannable, but otherwise very stable, laser frequencies (much narrower than the transition width for measurement time scales over typically the many seconds it takes to scan the two-photon resonance). This may be achieved with standard laser stabilization techniques, but is often costly, and can be challenging in a practical set-up. Because of this, we were able to obtain the highest quality polarization data with co-propagating beams, for which the line width is Doppler limited and the upper state hyperfine structure is unresolved. Finally, we point out that this is really a signal-to-noise issue, and the quietest and most stable polarization measurements can be made with relatively long dwell times at each frequency.

Even though measurements are frequently made with the excited level hyperfine structure unresolved, the influence of such structure is still not negligible in interpretation of the polarization signals. The present experiment provides a good illustration of this point. In the case of the $5s\ ^2S_{1/2} \rightarrow 5d\ ^2D_{5/2}$ transition, with the upper state hyperfine structure completely unresolved (Doppler width about 1.20 GHz, the largest excited hyperfine interval about 0.03 GHz), a constant polarization is read across the line profile. At the same time, calculations of individual $F \rightarrow F'$ transition amplitudes give identical P_L for all hyperfine structure (hfs) components of the line. Final state population ratios for parallel and perpendicular beam polarizations give $P_L = 0.143$, independent of F' . In this case, results are straightforward to interpret.

A different picture emerges for the $5s\ ^2S_{1/2} \rightarrow 5d\ ^2D_{3/2}$ transition. Here, the measured experimental polarization shows a significant asymmetry over the Doppler profile. This behaviour is illustrated in figure 5, along with the excitation line profile for the $F = 1, 2$ ground

hyperfine levels. With reference to figure 2, we attribute this effect to the hyperfine splitting of the upper level. As the laser frequency changes, excitation preference shifts sequentially from one $5d\ ^2D_{3/2}$ F' hyperfine level to another, and since individual hyperfine transition polarizations differ, a noticeable polarization slope results (in spite of a completely blended structure). We emphasize that, on the scale of the figure, there is no apparent asymmetry in the excitation profiles; the effect becomes apparent in the normalized difference represented by P_L .

We model this behaviour quantitatively by starting with a specific hyperfine component F in the ground level and calculating populations of various excited F' levels populated by two-photon excitation. The expected P_L differ dramatically for different F' and depends on detuning across the line profile. This behaviour is shown in the upper panel of figure 5 by the solid lines. In the case of the $F = 1$ initial level in ^{87}Rb the slope agreement is excellent. In the case of the $F = 2$ initial level the agreement is not quite as good. However, in this case the transition from the $F = 1$ initial level for the ^{85}Rb isotope is quite blended, reducing the slope substantially (this transition has an average linear polarization of about -0.7). If the Doppler widths were much greater than excited hyperfine energy intervals, then at any given frequency across a line profile, a completely hyperfine-structure-averaged result for P_L would have been obtained. In realistic experiments, even with the Doppler width clearly much larger than hyperfine level separations (as in figure 5), the previously discussed shift in excitation preference produces varying polarization readings as we scan over the Doppler profile of the line. We point out that we can quantitatively reproduce this effect by centring individual F' signal contributions at the proper frequencies and calculating the expected polarization slope over the line profile. The calculated polarization change across the line is almost linear with detuning and with slope agreeing well with the data. The calculated linear variation is shown by the line segments in the upper panel of figure 5. In the figure, the lines have been offset from the mean value of about -0.7 in order to compare more clearly with the experimental data. Note that in our other experiments using a similar approach, polarizations for individual hyperfine transitions were never determined because of the Doppler width limitation. However, the hyperfine-averaged values were precisely measured. This was accomplished by laser frequency scans over the entire unresolved hfs manifold, with points of data collection uniformly distributed over the line and correct interpretation of the polarization tilt effect. Finally, we point out that one can investigate individual hyperfine components, even in a Doppler-limited two-photon spectroscopy, if hyperfine intervals are large enough. One example of this is the atomic Cs $6s\ ^2S_{1/2} \rightarrow 8s\ ^2S_{1/2}$ two-photon transition; an experiment measuring the two-photon polarization-dependent excitation spectrum has recently been completed in our laboratory [26].

2.2. Reanalysis of experimental data and results

Our initial measurements on the $5s\ ^2S_{1/2} \rightarrow 5p\ ^2P_j \rightarrow 5d\ ^2D_{3/2}$ transitions in ^{87}Rb gave a value for the matrix-element ratio (defined in equation (7)) of 1.068(8). At that time, the overall agreement with theory was considered rather good, taking into account the complexity of the calculations and the experimental method, which had been applied to only a few cases. In addition, it was not possible to estimate, to equivalent precision, contributions to the ratio due to more energetically off-resonance transitions. However, we show in the following paragraphs that, when appropriate corrections are made, via reliable estimation of the coefficients p , q_1 and q_2 using recently available and refined theoretical matrix-element values, the agreement with theory becomes striking. In that case, the excited-state matrix-element ratio $R_2 = 1.098(9)$ is obtained as a direct theoretical prediction and $R_2 = 1.090(6)$ as a revised experimental

Table 1. Corrections to the parameter R for individual intermediate np multiplets. The correction is the sum of the contributions for each multiplet component.

np level	R contribution
6p	2.79×10^{-2}
7p	-3.82×10^{-3}
8p	-4.33×10^{-4}
9p	-1.92×10^{-4}
10p	-8.33×10^{-5}
11p	-4.69×10^{-5}
12p	-2.93×10^{-5}
13p	-1.93×10^{-5}
14p	-1.34×10^{-5}
15p	-9.79×10^{-6}
16p	-7.41×10^{-6}
17p	-5.75×10^{-6}
18p	-4.58×10^{-6}
19p	-3.69×10^{-6}
20p	-3.02×10^{-6}

result. Since the two-photon polarization spectroscopy resulted in an equally good agreement with other atoms and transitions, the results are compelling and illustrate the high accuracy of all-order relativistic calculations in alkali atoms. At the same time, the results speak equally favourably of the experimental technique.

In analysis of the data, polarization measurements are fit to the expressions in section 2 to extract a value of the basic parameter R . If contributions from energetically distant np levels are ignored, effectively setting p , q_1 and q_2 to zero, then the value $R = 1.066(6)$ is obtained. However, if the parameters are allowed to vary, then R , p , q_1 and q_2 become highly correlated, resulting in the parametric relation $R = 1.0661 + 36.3p - 0.48q_1 - 28.8q_2$. This expression, which efficiently summarizes the experimental results, then allows precise determination of R , assuming independent knowledge of p , q_1 and q_2 . To calculate these parameters, theoretical transition matrix elements, along with transition energies for the contributing levels, are needed. In obtaining calculated values, it is important to note that the contributions to the various parameters decrease rather quickly with principal quantum number n . The most important contributions are those from smaller n , particularly $n = 6, 7$ and 8 . For these, measured atomic energy level positions were used, and all-order j -dependent s-p and p-d transition matrix elements obtained from Safronova *et al* [30]. The all-order singles-doubles matrix elements agree with experimental data for the $5s$ - $5p$ transitions in Rb to better than 0.5%. For contributions from np levels with $n \geq 9$, energy level positions are generated from quantum defect expressions for the levels. The contribution to R for these levels is calculated from Dirac-Hartree-Fock transition matrix elements, which can have uncertainties on the order of 10-40%, in comparison with experimental values and all-order calculations.

The individual corrections to R for all levels up to $n = 20$ are summarized in table 1. To illustrate the total correction to R , the accumulated correction from table 1 is shown in figure 6 as a function of n . From figure 6, the overall correction is seen to be substantial, but to level off quickly for $n > 9$. In fact, even though the calculations extend to $n = 20$, the correction to R at the required precision is reached asymptotically by $n = 9$, with additional corrections for larger n well within the uncertainty in the measurements.

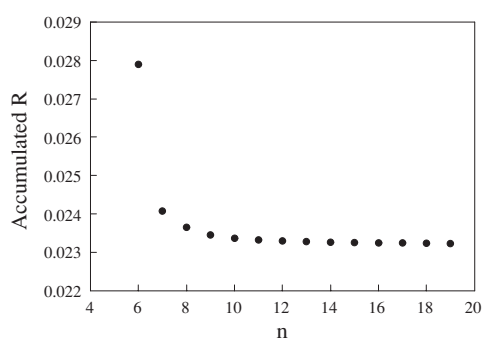


Figure 6. Accumulated matrix-element ratio R as a function of the maximum principal quantum number contributing to the sum.

To complete the analysis, recall that R is a product $R_2 R_1$ of ratios of matrix elements, as defined in equations (8) and (9), where the resonance transition matrix-element ratio has the well-known value of $R_1 = 0.999(1)$ as determined from precise measurements on this transition. This leads to an experimental value for the excited-state matrix-element ratio of $R_2 = 1.090(6)$. As discussed in the following section, recent precision calculations by Safronova give a theoretical value of $R_2 = 1.098(9)$ for this ratio, in excellent agreement with the experimental result. The agreement within the combined uncertainty is very satisfactory and suggests that yet sharper comparisons of relative matrix elements between experiment and theory are within reach.

3. Theoretical results

We carry out several calculations of the $5d^2 D_{3/2} - 5p^2 P_{3/2}$ and $5d^2 D_{3/2} - 5p^2 P_{1/2}$ electric-dipole matrix elements and the corresponding ratio R_2 in different approximations in order not only to provide a high-precision theoretical value for the ratio but also to estimate its accuracy. Firstly, we conduct a third-order many-body perturbation theory (MBPT) calculation following the method described in [31]. Secondly, we carry out the relativistic all-order calculation of the $5d^2 D_{3/2} - 5p^2 P_{3/2}$ and $5d^2 D_{3/2} - 5p^2 P_{1/2}$ matrix elements in single-double (SD) and SDpT (SD with partial triple excitations) approximations. Finally, we conduct semiempirical scaling of the final results in both cases to evaluate dominant part of the remaining correlation correction.

In the SD relativistic all-order method, single and double excitations of Dirac–Hartree–Fock (DHF) wavefunctions are included to all orders of perturbation theory. The single and double excitation coefficients are obtained as the iterative solutions of the all-order equations in the finite basis set. The basis set, used in the present calculation, consists of the single-particle states, which are linear combinations of B-splines [32]. The single-particle orbitals are defined on a nonlinear grid and are constrained to a spherical cavity. In the SDpT method, specific subset of the triple contributions is included perturbatively. We refer the reader to [33–35] for the detailed description of the SD all-order method and its extensions. The breakdown of the correlation contributions to the $5d^2 D_{3/2} - 5p^2 P_{3/2}$ and $5d^2 D_{3/2} - 5p^2 P_{1/2}$ matrix elements shows that most of the correlation correction comes from only one term that contains only single valence excitation coefficients. All other terms are at least an order of magnitude smaller than the dominant term. We also observe some cancellation between the remaining terms. As the particular subset of triples that is included in the SDpT calculation specifically corrects the

Table 2. Lowest-order (DHF), third-order MBPT, all-order results for $5d\ ^2D_{3/2}-5p\ ^2P_{3/2}$ and $5d\ ^2D_{3/2}-5p\ ^2P_{1/2}$ electric-dipole matrix elements divided by the corresponding values of the C_1 reduced matrix elements, where C_1 are the normalized spherical harmonics. The *ab initio* all-order values calculated in single-double (SD) approximation and with partial inclusion of the triple excitations are given. The corresponding scaled values are given in rows labelled ‘SD scaled’ and ‘SDpT scaled’. The ratio R_2 , defined by equation (9), is also listed.

	$5d^2D_{3/2}-5p^2P_{3/2}$	$5d^2D_{3/2}-5p^2P_{1/2}$	R_2
DHF	0.3034	0.2115	1.434
Third order	1.1785	1.0588	1.113
All order			
SD	1.5394	1.4138	1.089
SDpT	1.3610	1.2404	1.097
SD scaled	1.2882	1.1707	1.100
SDpT scaled	1.2638	1.1457	1.103

single valence excitation coefficients, we expect SDpT calculation to be more accurate than the SD calculation. The semiempirical scaling procedure is described, for example, in [35] and references therein. It is specifically aimed at the correction of the single valence excitation coefficients and energies. Therefore, it is particularly suited for this specific calculation as it estimates the missing part of the overwhelmingly dominant contribution. We carry out the scaling procedure for both SD and SDpT calculations. The scaling factors (which are the ratios of the all-order ‘experimental’ to theoretical correlation energies for the specific state) are different in SD and SDpT cases. The ‘experimental’ correlation energy is defined as a difference between the experimental energy and the DHF value.

Lowest-order (DHF), third-order MBPT and all-order results for the $5d\ ^2D_{3/2}-5p\ ^2P_{3/2}$ and $5d\ ^2D_{3/2}-5p\ ^2P_{1/2}$ electric-dipole matrix elements and their ratio R_2 are given in table 2. All matrix elements are divided by the corresponding values of the C_1 reduced matrix elements, where C_1 are the normalized spherical harmonics, to make the relativistic effects apparent. The *ab initio* all-order values calculated in the SD approximation and with partial inclusion of the triple excitations (SDpT) are given in rows labelled SD and SDpT, respectively. The corresponding scaled values are given in rows labelled ‘SD scaled’ and ‘SDpT scaled’. Some of the values have been previously published in [30]. We included the contribution from the higher partial waves ($l > 6$) into the current calculation of the *ab initio* values which was not included in [30]. It was found to be on the order of 1%. We see from table 2 that the correlation correction to $5d\ ^2D_{3/2}-5p\ ^2P_{3/2}$ and $5d\ ^2D_{3/2}-5p\ ^2P_{1/2}$ electric-dipole matrix elements is extremely large. In fact, the all-order values are four times as large as the lowest-order DHF results. In contrast, similar all-order calculation for the $5s\ ^2S_{1/2} \rightarrow 5p\ ^2P_{1/2}$ principal transition in Rb differs from the DHF result by only 14% [30]. Moreover, the DHF value for the ratio of the $5d\ ^2D_{3/2}-5p\ ^2P_{3/2}$ and $5d\ ^2D_{3/2}-5p\ ^2P_{1/2}$ matrix elements differs from the all-order value by 30% while the corresponding difference for the $5s\ ^2S_{1/2} \rightarrow 5p\ ^2P_{3/2}$ and $5s\ ^2S_{1/2} \rightarrow 5p\ ^2P_{1/2}$ matrix elements is less than 0.1%. Therefore, these particular transitions represent an excellent test of the high-precision methods of the current state-of-the-art atomic theory.

As expected, we find large discrepancies even between the third-order and all-order results demonstrating large contributions from fourth and higher orders (that can be estimated as the difference between the third-order and all-order results). The inclusion on the triple excitations still changes the values of the matrix elements by 13–14%. However, the scaling procedure for SD and SDpT values produces results that are consistent to 2%.

Table 3. Breit correction to the lowest-order (DHF), third-order MBPT, all-order (SDpT) results for the $5d\ ^2D_{3/2}-5p\ ^2P_{3/2}$ and $5d\ ^2D_{3/2}-5p\ ^2P_{1/2}$ electric-dipole matrix elements divided by the corresponding values of the C_1 reduced matrix elements and their ratio R_2 .

	$5d\ ^2D_{3/2}-5p\ ^2P_{3/2}$	$5d\ ^2D_{3/2}-5p\ ^2P_{1/2}$	R_2
Lowest order			
No Breit	0.3034	0.2115	1.434
With Breit	0.3088	0.2183	1.414
Breit correction	0.0055	0.0069	-0.020
	1.8%	3.1%	
Third order			
No Breit	1.1785	1.0588	1.113
With Breit	1.1877	1.0698	1.110
Breit correction	0.0092	0.0110	-0.003
	0.8%	1.0%	
All order			
No Breit	1.3610	1.2404	1.097
With Breit	1.3703	1.2515	1.095
Breit correction	0.0093	0.0111	-0.002
	0.7%	0.9%	

We also investigated the effect of the Breit interaction to the values of the $5d\ ^2D_{3/2}-5p\ ^2P_{3/2}$ and $5d\ ^2D_{3/2}-5p\ ^2P_{1/2}$ matrix elements and their ratio R_2 . The Breit interaction arises from the exchange of a virtual photon between atomic electrons. The complete expression for the Breit matrix elements is given in [36]. To calculate the correction to the matrix elements arising from the Breit interaction, we modified the generation of our finite B-spline basis set to intrinsically include the Breit interaction on the same footing as the Coulomb interaction and repeated both third-order and all-order calculations with the modified basis set. Such a procedure does not include a class of the Breit correction contributions referred to in [37] as ‘two-body’ Breit contribution (the Breit interaction is a two-particle interaction just as the Coulomb interaction, the separation of the Breit contribution to ‘one-body’ and ‘two-body’ parts results from transforming the Breit operator in second quantization to normal form as described in [37].) The uncertainty resulting from the omission of the ‘two-body’ part of the Breit interaction was discussed in detail in [38]. It was shown that it is unlikely to exceed the one-body correction. The summary of the results for the Breit correction, that is defined as the difference between the same calculation with and without the inclusion of the Breit interaction into the basis set functions, is given in table 3. We find that effect of the Breit interaction is unusually large (2–3%) at the DHF level but is reduced to less than 1% with the inclusion of the correlation. We find very small differences between the Breit correction to third-order and all-order values leading to conclusion that our calculation of the ‘one-body’ part of the Breit interaction is accurate. The Breit correction reduces the value of the R_2 ratio by 0.2%. It is significantly smaller than the uncertainty in our calculation of the Coulomb correlation correction.

We take the SD-scaled values corrected for the Breit interaction as our final numbers based on the comparisons of similar calculations in alkali-metal atoms with experiment [35, 30, 38]. There are three sources of the uncertainty in our calculation of the ratio R_2 : the uncertainty in our calculation of the dominant term that can be accounted by the semiempirical scaling, the remaining uncertainty in the Coulomb correlation and the uncertainty in the Breit interaction caused by the omission of the ‘two-body’ part of the Breit correction. We take the first uncertainty contribution to be the spread of the SDpT, SD-scaled and SDpT-scaled values for

Table 4. Comparison of the experimental and theoretical values for the ratio R_2 of the $5d\ ^2D_{3/2}-5p\ ^2P_{3/2}$ and $5d\ ^2D_{3/2}-5p\ ^2P_{1/2}$ reduced electric-dipole matrix elements divided by the corresponding values of the C_1 reduced matrix elements. Theory and experiment (Exp.) refer to the present paper.

	$5d\ ^2D_{3/2}-5p\ ^2P_{3/2}$	$5d\ ^2D_{3/2}-5p\ ^2P_{1/2}$	R_2
Theory	1.298	1.182	1.098(9)
Exp.			1.090(6)
Reference [25]	1.022	0.900	1.135

the ratio (0.006). The remaining uncertainty in the Coulomb correlation correction should not exceed the uncertainty of the dominant term and is taken to be the same (0.006) which is most likely an overly pessimistic assumption. The uncertainty in the Breit interaction is taken to be the Breit correction itself as discussed in [38]. Adding the above uncertainties in quadrature yields the final uncertainty of the theoretical ratio to be 0.009. The comparison of our final theory values with the current experimental value for the ratio R_2 and other theoretical calculations is given in table 4. Our theory value for the ratio agrees with the experimental result within the uncertainty of the calculations. The theoretical calculation of [25] is a third-order MBPT calculation with some addition of the fourth-order terms (that accounts for the discrepancy of the results of [25] without third-order calculation). We expect our values to be more accurate owing to more complete treatment of the correlation correction. We note that the current all-order calculation is the most accurate calculation of these matrix elements to date.

4. Conclusions

A combined experimental study of relative transition matrix elements associated with the $5s\ ^2S_{1/2} \rightarrow 5p\ ^2P_j \rightarrow 5d\ ^2D_{j'}$ transition in ^{87}Rb is reported. The experimental results consist of measurements of the spectral, temperature and initial hyperfine level dependence of the polarization-dependent excitation of the final $5d\ ^2D_{j'}$ levels ($j' = 3/2, 5/2$). The effects are manifested through alignment and population transfer from the initially prepared $5d\ ^2D_{j'}$ levels to the $6p\ ^2P_j \rightarrow 5s\ ^2S_{1/2}$ experimental observation channel. The results illustrate important systematic effects which can influence the precision of matrix elements extracted from the data. Further, measured matrix elements reported in an earlier publication are reanalysed using recently available matrix-element calculations to correct for the systematic influence of energetically distant transitions. The resulting experimental and theoretical excited-state matrix-element ratios are in excellent agreement.

Acknowledgments

The financial support of the National Science Foundation, the Research Corporation (CC6119) and Central Michigan University is greatly appreciated. Part of this research was performed under the sponsorship of the US Department of Commerce, National Institute of Standards and Technology. We acknowledge the contributions of M Rosu to the experimental aspects of this research.

References

- [1] Molish F and Oehry B P 1998 *Radiation Trapping in Atomic Vapours* (Oxford: Clarendon)
 Corney A 1998 *Atomic and Laser Spectroscopy* (Oxford: Clarendon)

- [2] Wiese W L, Smith M W and Glennon B M 1966 *Atomic Transition Probabilities* vols 1–2, Natl. Bur. Stand. (U.S.) Circ. No. 4 (Washington, DC: US Govt Printing Office)
- [3] Radzig A A and Smirnov B M 1985 *Reference Data on Atoms, Molecules and Ions* (Berlin: Springer)
- [4] Cohen-Tannoudji C, Dupont-Roc J and Grynberg G 1992 *Atom–Photon Interactions: Basic Processes and Applications* (New York: Wiley)
- [5] Metcalf H J and van der Straten P 1999 *Laser Cooling and Trapping* (New York: Springer)
- [6] Mihalas D 1970 *Stellar Atmospheres* (San Francisco: Freeman)
- [7] McAlexander W I, Abraham E R I and Hulet R G 1996 *Phys. Rev. A* **54** R5
- [8] McAlexander W I, Abraham E R I, Ritchie N W M, Williams C J, Stoof H T C and Hulet R G 1995 *Phys. Rev. A* **51** R871
- [9] Oates C W, Vogel K R and Hall J L 1996 *Phys. Rev. Lett.* **76** 2866
- [10] Volz U, Jajerus M, Liebel H, Schmitt A and Schmoranzler H 1996 *Phys. Rev. Lett.* **76** 2862
- [11] Volz U and Schmoranzler H 1996 *Phys. Scr.* T **65** 48
- [12] Tanner C E, Livingston A E, Rafac R J, Serpa F G, Kukla K W, Berry H G, Young L and Kurtz C A 1992 *Phys. Rev. Lett.* **69** 2765
- [13] Rafac R J, Tanner C E, Livingston A E, Kukla K W, Berry J G and Kurtz C A 1994 *Phys. Rev. A* **50** R1976
- [14] Young L, Hill W T III, Sibener S J, Price S D, Tanner C E, Wieman C E and Leone S R 1994 *Phys. Rev. A* **50** 2174
- [15] Rafac R J and Tanner C E 1998 *Phys. Rev. A* **58** 1087
- [16] Rafac R J, Tanner C E, Livingston A E and Berry H G 1999 *Phys. Rev. A* **60** 3648
- [17] Vasilyev A A, Savukov I M, Safronova M S and Berry H G 2002 *Phys. Rev. A* **66** 020101
- [18] Markhotok A, Bayram S B, Sieradzan A and Havey M D 2002 *J. App. Phys.* **92** 1613
- [19] Ekstrom C R, Schmiedmayer J, Chapman M S, Hammond T D and Pritchard D E 1995 *Phys. Rev. A* **51** 3883
- [20] Jones K M, Julienne P S, Lett P D, Phillips W D, Tiesinga E and Williams C J 1996 *Europhys. Lett.* **35** 85
- [21] Wang H, Li J, Wang X T, Williams C J, Gould P L and Stwalley W C 1997 *Phys. Rev. A* **55** R1569
- [22] Safronova M S and Clark C W 2004 *Phys. Rev. A* **69** 040501(R)
- [23] Meyer R P, Beger A I and Havey M D 1997 *Phys. Rev. A* **55** 38780
- [24] Beger A I, Havey M D and Meyer R P 1997 *Phys. Rev. A* **55** 3780
- [25] Bayram S B, Havey M, Rosu M, Sieradzan A, Derevianko A and Johnson W R 2000 *Phys. Rev. A* **61** 050502
- [26] Sieradzan A, Havey M D and Safronova M S 2004 *Phys. Rev. A* **69** 022502
- [27] Havey M D 1998 *Phys. Lett. A* **240** 219
- [28] Loudon R 1992 *Quantum Theory of Light* 2nd edn (Oxford: Oxford University Press)
- [29] Varshalovich D A, Moskalev A N and Khersonskii V K 1988 *Quantum Theory of Angular Momentum* (Singapore: World Scientific)
- [30] Safronova M S, Williams C J and Clark C W 2004 *Phys. Rev. A* **69** 022509
- [31] Johnson W R, Liu Z W and Sapirstein J 1996 *At. Data Nucl. Data Tables* **64** 279
- [32] Johnson W, Blundell S and Sapirstein J 1998 *Phys. Rev. A* **37** 307
- [33] Blundell S A, Johnson W R and Sapirstein J 1991 *Phys. Rev. A* **43** 3407
- [34] Safronova M S, Derevianko A and Johnson W R 1998 *Phys. Rev. A* **58** 1016
- [35] Safronova M S, Johnson W R and Derevianko A 1999 *Phys. Rev. A* **60** 4476
- [36] Johnson W, Blundell S and Sapirstein J 1998 *Phys. Rev. A* **37** 2764
- [37] Derevianko A 2002 *Phys. Rev. A* **65** 012106
- [38] Kreuter A *et al* 2005 *Phys. Rev. A* **71** 032504